


FBXW7 modulates malignant potential and cisplatin-induced apoptosis in cholangiocarcinoma through NOTCH1 and MCL1

Akiko Mori¹ | Kunihiro Masuda¹  | Hideo Ohtsuka¹ | Masahiro Shijo¹ | Kyohei Ariake¹ | Koji Fukase¹ | Naoaki Sakata¹ | Masamichi Mizuma¹ | Takanori Morikawa¹ | Hiroki Hayashi¹ | Kei Nakagawa¹ | Fuyuhiko Motoi¹ | Takeshi Naitoh¹ | Fumiyoshi Fujishima² | Michiaki Unno¹

¹Department of Surgery, Tohoku University Graduate School of Medicine, Sendai, Japan

²Department of Pathology, Tohoku University Hospital, Sendai, Japan

Correspondence

Kunihiro Masuda, Department of Surgery, Tohoku University Graduate School of Medicine, Sendai, Japan.
Email: k-masuda0911@surg.med.tohoku.ac.jp

Funding information

Japan Society for the Promotion of Science, Grant/Award Number: 16K19910 and 26861058

The ubiquitin ligase F-box and WD repeat domain-containing 7 (FBXW7) is responsible for degrading diverse oncoproteins and is considered a tumor suppressor in many human cancers. Inhibiting FBXW7 enhances the malignant potential of several cancers. In this study, we aimed to investigate the role of FBXW7 in cholangiocarcinoma. We found that FBXW7 expression was associated with clinicopathological outcomes in cholangiocarcinoma patients. Both disease-free and overall survival were significantly worse in the low-FBXW7 group than in the high-FBXW7 group ($P = .001$ and $P < .001$, respectively). Multivariate analysis with the Cox proportional hazards model indicated that FBXW7 was the most important independent prognostic factor for disease-free ($P = .006$) and overall ($P = .0004$) survival. We also showed that the two FBXW7 substrates, NOTCH1 and myeloid cell leukemia sequence 1 (MCL1), regulate cholangiocarcinoma progression. Depletion of FBXW7 resulted in NOTCH1 accumulation and increased cholangiocarcinoma cell migration and self-renewal. Interestingly, when cells were stimulated with cis-diamminedichloridoplatinum(II) (cisplatin), FBXW7 suppression induced MCL1 upregulation, which reduced the sensitivity of cholangiocarcinoma cells to apoptosis, indicating that FBXW7-mediated ubiquitylation is context-dependent. These results indicate that FBXW7 modulates the malignant potential of cholangiocarcinoma through independent regulation of NOTCH1 and MCL1.

KEYWORDS

cholangiocarcinoma, cisplatin, FBXW7 protein, myeloid cell leukemia sequence 1 protein, NOTCH1 protein

1 | INTRODUCTION

Cholangiocarcinoma is a rare and aggressive malignancy originating in the epithelium of the bile duct. East and South Asia have

the highest incidences of CC, although those in Europe, North America, and Australia have increased in recent decades.¹ Chronic inflammation and bile stasis in the biliary tract, such as from gallstones, chronic hepatitis, primary sclerosing cholangitis, and liver fluke

Abbreviations: CC, cholangiocarcinoma; CDDP, cis-diamminedichloridoplatinum(II) (cisplatin); CSC, cancer stem cell; DFS, disease-free survival; FBXW7, F-box and WD repeat domain-containing 7; GEM, gemcitabine; MCL1, myeloid cell leukemia sequence 1; NICD, NOTCH intracellular domain; OS, overall survival; qPCR, quantitative RT-PCR; T-ALL, T-cell acute lymphoblastic leukemia.

This is an open access article under the terms of the Creative Commons Attribution-NonCommercial License, which permits use, distribution and reproduction in any medium, provided the original work is properly cited and is not used for commercial purposes.

© 2018 The Authors. *Cancer Science* published by John Wiley & Sons Australia, Ltd on behalf of Japanese Cancer Association.

infection, are considered specific risk factors for CC.^{2,3} Because of its insidious nature, CC is usually diagnosed at an advanced stage and has a poor prognosis. Complete surgical resection is the most effective therapy for CC⁴; however, this does not significantly improve prognosis, especially in cases with lymph node metastasis and perineural invasion.⁵ The current standard for chemotherapy in advanced stages of CC is the combination of GEM and CDDP.⁶ The clinical efficacy of this regimen is limited, with a median survival of 11 months.⁷ Therefore, clarification of the molecular mechanisms of CC is urgently needed for the development of more effective therapies.

F-box and WD repeat domain-containing 7 (FBXW7) (also known as Fbw7, SEL-10, hCdc4, or hAgo) is a member of the F-box family of proteins and was first identified in *Caenorhabditis elegans* as a negative regulator of the signaling protein NOTCH (LIN-12).⁸ FBXW7 functions as the substrate-recognition subunit of the S-phase kinase-associated protein 1/Cullin 1/F-box protein E3 ubiquitin ligase complex, which targets various mammalian oncoproteins that promote cell-cycle progression and regulate proliferation, growth, and apoptosis for proteasomal degradation.⁹⁻¹² FBXW7 substrates include cyclin E,¹³ NOTCH,¹⁴ mTOR,^{15,16} MCL1,¹² c-Myc,^{17,18} and c-Jun.¹⁹ Given its role in the degradation of these oncoproteins, FBXW7 is considered a tumor suppressor, and its deficiency leads to tumorigenesis.⁹ Indeed, loss-of-function mutations in FBXW7 are found in breast and colorectal cancers,²⁰ T-ALL,^{9,21} and CC,²² with an especially high frequency of mutation observed in CC patients (5%-35%).²²⁻²⁴ FBXW7 has 3 functional domains that are critical to its function as a ubiquitin ligase, and the WD40 domain includes 3 arginine residues that are mutational hot spots in cancer.²⁵ However, one study found that in pancreatic ductal adenocarcinoma, FBXW7 was rarely mutated, although its protein levels were significantly reduced through a mechanism involving activated Ras/Raf/MAPK kinase/ERK signaling, with a resultant increase in tumorigenic potential.²⁶

The NOTCH signaling pathway is evolutionarily conserved and plays an important role in cell proliferation, differentiation, self-renewal, and migration.^{27,28} NOTCH1 signaling is activated by the binding of the NOTCH ligand to its cognate receptor,²⁸ which is then cleaved by γ -secretase and functions as a NOTCH1 intracellular domain. This enters the nucleus and regulates the transcription of target genes.²⁸ NOTCH1 intracellular domain is degraded by FBXW7-mediated ubiquitylation.²⁸ NOTCH signaling is aberrantly activated in various malignancies.²⁹⁻³² In T-ALL, NOTCH signaling is activated by mutations in either NOTCH1 and/or FBXW7 and is associated with poor prognosis.³³ Moreover, it has been shown that NOTCH signaling induces a biliary differentiation program in hepatocytes or hepatic progenitor cells, leading to intrahepatic CC.³⁴ Thus, NOTCH1 is closely associated with both FBXW7 and CC. In fact, we previously reported that aberrant NOTCH signaling in CC might be an indicator of poor survival and that inhibiting NOTCH signaling with agents such as γ -secretase inhibitor IX could be a novel strategy for targeting cells with CSC-like properties.³⁵

Cholangiocarcinoma cells are resistant to chemotherapeutic agents such as CDDP, accounting for the poor prognosis of CC.^{7,36} Several studies have described the relationship between the mechanism of CDDP resistance and the accumulation of MCL1.³⁶⁻³⁸ Despite the importance of MCL1 in several cancers, the relationship between the FBXW7/MCL1 pathway and CDDP-induced apoptosis in CC has not been previously investigated, and the association between FBXW7 and MCL1 in CC remains unknown.

We aimed to address these questions in the present study by first investigating the relationship between FBXW7 expression and clinicopathological outcomes in CC patients to assess the prognostic value of FBXW7 expression. In addition, we examined the possible mechanisms underlying CC progression by exploring the expression of FBXW7 and its substrates.

2 | MATERIALS AND METHODS

2.1 | Patients and specimens

Consecutive patients with surgically resected CC (n = 154), treated at Tohoku University Hospital (Sendai, Japan) between 2008 and 2013, were examined in this study. Patients that died in the hospital and those in which FBXW7 could not be evaluated were excluded. Histological differentiation and tumor staging were based on the 7th edition of the UICC classification. This study was authorized by the Institutional Review Board of Tohoku University (2017-1-329), and all patients provided written, informed consent. The median age of the patients was 68.5 years (range, 42-82 years). There were 105 male and 49 female patients; 96 had perihilar CC, and 58 had distal CC. Lymph node metastases were observed in 74 patients (48.1%) and distant metastases in 18 patients (11.7%). In 135 patients (87.7%), neural invasion was detected. Curative resection with negative histological margins was achieved in 127 patients (82.5%). In total, 110 patients (71.4%) received adjuvant chemotherapy.

2.2 | Immunohistochemistry

Immunohistochemistry was carried out using Abs against FBXW7 (3D1, 1:200 dilution; Abnova, Taipei, Taiwan) and MCL1 (1:500 dilution; Cell Signaling Technology, Danvers, MA, USA). Specimens were fixed in 10% formalin at 20-25°C, embedded in paraffin, and cut into 3- μ m-thick sections that were placed on glue-coated glass slides. The sections were deparaffinized in xylene and rehydrated in a graded series of alcohol and distilled water. Endogenous peroxidase activity was blocked with 3% H₂O₂ for 10 minutes. Antigen retrieval was undertaken by boiling the slides in citrate buffer (pH 6.0). The sections were incubated with primary Abs for 16 hours at 4°C. Secondary Ab reactions were carried out for 30 minutes using EnVision FLEX/HRP (Dako, Glostrup, Denmark), and the sections were visualized by treatment with 3,3'-diaminobenzidine tetrachloride and 30% H₂O₂ in 0.05 mol/L Tris buffer (pH 7.6) followed by counterstaining with hematoxylin.

2.3 | Assessment of FBXW7 expression

Given the heterogeneity in FBXW7 immunostaining, *H* scoring was used for evaluation. The percentage of immunostaining and staining intensity (0, negative; 1+, weak; 2+, moderate; and 3+, strong) was recorded (Figure S1). An *H* score was calculated using the following formula: $H \text{ score} = (\% \text{ of cells of weak intensity} \times 1) + (\% \text{ of cells of moderate intensity} \times 2) + (\% \text{ of cells of strong intensity} \times 3)$. The maximum *H* score was 300, corresponding to 100% of cells with strong intensity.³⁹ Receiver operating characteristic curve analysis was undertaken to obtain an optimal cut-off score to analyze and distinguish tumors based on FBXW7 expression. For receiver operating characteristic curve analysis, we divided patients into two groups based on specific survival (dead and alive). We defined an *H* score > 110 as high expression and an *H* score ≤ 110 as low expression. The evaluation was carried out by two investigators (A.M. and F.F.) who were blinded to patients' clinical information.

2.4 | Cell culture and drug treatment

RBE, HuCCT1, and TFK-1 human CC cell lines were purchased from RIKEN BioResource Center (Tsukuba, Japan) and cultured in RPMI-1640 medium (Sigma-Aldrich, St. Louis, MO, USA) supplemented with 10% heat-inactivated FBS (Sigma-Aldrich) and 1% penicillin/streptomycin (Thermo Fisher Scientific, Waltham, MA, USA) at 37°C and 5% CO₂. Cisplatin was purchased from Nippon Kayaku (Tokyo, Japan) and diluted with cell culture medium before use in *in vitro* experiments.

2.5 | Short interfering RNA transfection

The sense and antisense siRNA oligonucleotides used in this experiment are listed in Table S1 and were purchased from Thermo Fisher Scientific. Subconfluent cells were transfected with siRNAs using Lipofectamine RNAiMAX (Thermo Fisher Scientific) according to the manufacturer's protocol.

2.6 | Short hairpin RNA transfection

To generate stably transfected cell lines, DNA oligonucleotides encoding shRNAs directed against *FBXW7* were annealed and subcloned into the *Bam*HI and *Hind*III sites of the pBAsi-hU6 Neo DNA vector (Takara Bio, Otsu, Japan). The sense and antisense shRNA sequences used in this experiment are listed in Table S2. RBE cells were transfected with *FBXW7* shRNA using Lipofectamine LTX Reagent with Plus (Thermo Fisher Scientific) according to the manufacturer's protocol. The pBAsi-hU6 Neo DNA negative control vector (Takara Bio), encoding an shRNA sequence not found in the human genome database, was used as a control. Transfected clones were selected using G418 (1000 µg/mL) for 3 weeks, and single clones were selected using the limited dilution method. *FBXW7* silencing was evaluated by qRT-PCR and immunoblotting.

2.7 | Quantitative RT-PCR

For mRNA quantification, total RNA was isolated using Nucleospin RNA II (Takara Bio). RNA was quantified with a Nanodrop spectrophotometer (Thermo Fisher Scientific). cDNA was synthesized from 1.5 µg total RNA using PrimeScript RT Master Mix (Takara Bio), and qPCRs were carried out on a StepOnePlus Real-time PCR system (Thermo Fisher Scientific) using SYBR Premix Ex Taq II (Tli RNaseH Plus; Takara Bio). *GAPDH* mRNA was used as an internal reference. The primers used in this experiment are listed in Table S3. Relative transcript levels were calculated with the 2^{-ΔΔCT} method.

2.8 | Immunoblotting

Cells were lysed in radioimmunoprecipitation assay buffer (Thermo Fisher Scientific) with complete protease and phosphatase inhibitors (Roche Diagnostics, Indianapolis, IN, USA). For immunoblotting, cell lysates were loaded on 5% and 7.5% polyacrylamide gels, separated by SDS-PAGE, and then transferred to a PVDF membrane using a Trans-Blot Turbo blotting system (Bio-Rad, Hercules, CA, USA). The membrane was blocked with SuperBlock (TBS) Blocking Buffer (Thermo Fisher Scientific) for 90 minutes at 20–25°C. Signals were detected using Clarity Western ECL Substrate (Bio-Rad) according to the manufacturer's instructions. Antibodies used in this experiment are listed in Table S4. The densitometric analysis was undertaken using ImageJ software (<http://imagej.nih.gov/ij/>). Arbitrary densitometric units of the proteins of interest were normalized to those of *GAPDH*.

2.9 | Colony formation assay

Cells were seeded in 6-well plates at 1 × 10³ cells/well and cultured for 10 days before being fixed in 99.5% ethanol for 30 minutes and stained with 1% crystal violet solution for 30 minutes. The number and sizes of colonies were recorded, and results are reported as the mean of 3 independent experiments performed in triplicate.

2.10 | Wound healing assay

Cells were seeded in a 6-well plate and grown until 90%–100% confluence. Monolayers were scratched with a 200-µL sterile pipette tip to create an artificial wound, which was photographed at 0 and 20 hours. Cell motility was evaluated by measuring the change in the migration area. Results are presented as the mean of 3 independent experiments performed in triplicate.

2.11 | Migration assay

Transwell assays were carried out using a 24-well cell migration chamber kit (pore size = 8 µm; Millipore, Billerica, MA, USA). Cells were resuspended in serum-free medium and transferred to the upper chamber (3 × 10⁵ cells in 300 µL), while medium containing stimulant

Factors		FBXW7 expression		P value ^a
		High (n = 37)	Low (n = 117)	
Age, year		71 (42-80)	67 (46-82)	.312
Sex	Male	23	82	.367
	Female	14	35	
Location	Perihilar	24	72	.716
	Distal	13	45	
Neoadjuvant chemotherapy	No	32	101	.98
	Yes	5	16	
UICC-G	1, 2	32	106	.54
	3	4	9	
UICC-pT	1, 2	20	58	.635
	3, 4	17	59	
UICC-pN	0	23	57	.154
	1	14	60	
UICC-pM	0	34	102	.437
	1	3	15	
Nodal invasion	Negative	7	10	.079
	Positive	30	107	
Vessel invasion	Negative	6	8	.084
	Positive	31	109	
Neural invasion	Negative	6	13	.411
	Positive	31	104	
Curative resection	R0	30	97	.799
	R1 or 2	7	20	
Adjuvant chemotherapy	No	13	31	.311
	Yes	24	86	

TABLE 1 Correlation analysis between FBXW7 expression and clinicopathological characteristics in 154 cholangiocarcinoma patients

^a χ^2 test.

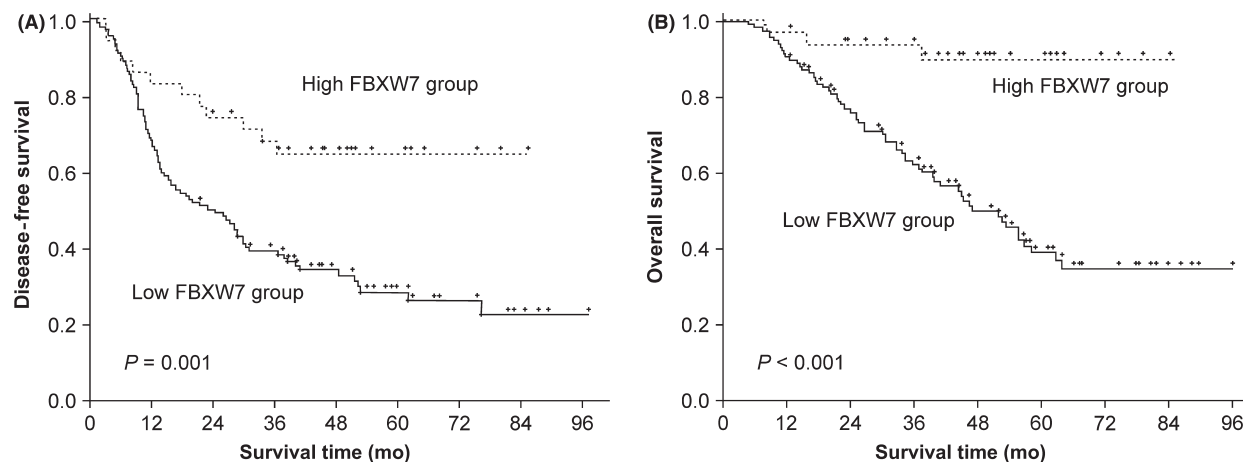


FIGURE 1 Association between FBXW7 expression and cholangiocarcinoma patient survival. A, Kaplan–Meier analysis of disease-free survival according to FBXW7 expression levels. B, Overall survival according to FBXW7 expression levels. Dotted and solid lines indicate high and low FBXW7 expression groups, respectively. P values were determined with the log-rank test

(10% FBS) was added to the lower chamber. After incubation for 24 hours, cells that had migrated to the lower chamber were detached and stained according to the manufacturer's protocol.

Migrated cells were detected with a fluorescence microplate reader. Results are presented as the mean of 3 independent experiments performed in triplicate.

2.12 | Apoptosis assay

To detect apoptosis, cells treated with CDDP (50 $\mu\text{mol/L}$) for 24 hours and with GEM (0.1-10 $\mu\text{mol/L}$) for 48 hours were stained with propidium iodide and annexin V-FITC (BD Biosciences, Franklin Lakes, NJ, USA) according to the manufacturer's instructions. Stained cells were sorted on a FACSVerse system (BD Biosciences). Cells that were positive only for annexin V-FITC were counted as apoptotic cells. Results are presented as the mean of 3 independent experiments performed in triplicate.

2.13 | Statistical analysis

Unless otherwise indicated, data are expressed as the mean \pm SE. Differences between two groups were evaluated with the *t* test.

The χ^2 test was used to compare categorical variables, and the Kaplan-Meier method was used to generate survival curves. Associations between clinicopathological factors and FBXW7 expression were assessed based on Pearson's correlation coefficients. Data were analyzed with JMP Pro version 11.2.0 software (SAS Institute, Cary, NC, USA). *P* < .05 was considered statistically significant.

3 | RESULTS

3.1 | FBXW7 expression is not correlated with clinicopathological features of CC

To investigate the relationship between FBXW7 expression and clinicopathological characteristics of CC, the 154 CC patients were classified into groups with relatively high FBXW7 expression (*H* score > 110, *n* = 37) and

TABLE 2 Univariate and multivariate analyses of prognostic factors for disease-free survival (A) and overall survival (B)

Prognostic factor	Univariate analysis	Multivariate analysis		
	<i>P</i> value	RR	95% CI	<i>P</i> value
(A) Disease-free survival				
FBXW7 (low vs high)	.0010	2.244	1.25-4.417	.0060*
Age, years (<65 vs \geq 65)	.1550	–	–	–
Gender (male vs female)	.5970	–	–	–
Location (perihilar vs distal)	.5700	–	–	–
Neoadjuvant chemotherapy (with vs without)	.6010	–	–	–
UICC-G (1/2 vs 3)	.9930	–	–	–
UICC-pT (T1/2 vs T3/4)	.0020	0.657	0.419-1.021	.0620
UICC-pN (1 vs 0)	<.0001	2.624	1.680-4.178	<.0001*
Node invasion (1 vs 0)	.0004	2.748	0.627-15.842	.1930
Vessel invasion (1 vs 0)	.0100	1.933	0.398-7.348	.3910
Nerve invasion (1 vs 0)	.0010	2.275	0.751-9.211	.1590
Adjuvant chemotherapy (with vs without)	.0010	1.015	0.578-1.881	.9610
(B) Overall survival				
FBXW7 (low vs high)	.0001	5.172	1.889-21.339	.0004*
Age (<65 vs \geq 65)	.3850	–	–	–
Gender (male vs female)	.4800	–	–	–
Location (perihilar vs distal)	.4690	–	–	–
Neoadjuvant chemotherapy (with vs without)	.3480	–	–	–
UICC-G (1/2 vs 3)	.8990	–	–	–
UICC-pT (T1/2 vs T3/4)	.0010	0.549	0.311-0.949	.0320*
UICC-pN (1 vs 0)	<.0001	2.514	1.427-4.549	.0010*
UICC-pM (1 vs 0)	<.0001	2.179	1.09-4.115	.0290*
Node invasion (1 vs 0)	.0130	1.248	0.300-6.668	.7740
Vessel invasion (1 vs 0)	.0510	–	–	–
Nerve invasion (1 vs 0)	.0290	1.037	0.323-4.46	.9560
Curative resection (R0 vs R1/2)	.0290	0.577	0.314-1.132	.1060
Adjuvant chemotherapy (with vs without)	.0050	1.011	0.502-2.213	.9770

**P* < .05.

–, not applicable; CI, confidence interval; RR, relative risk.

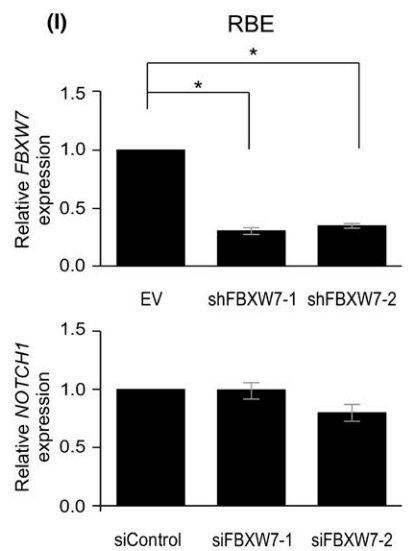
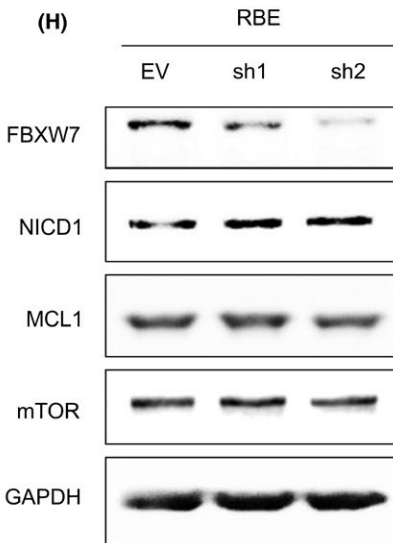
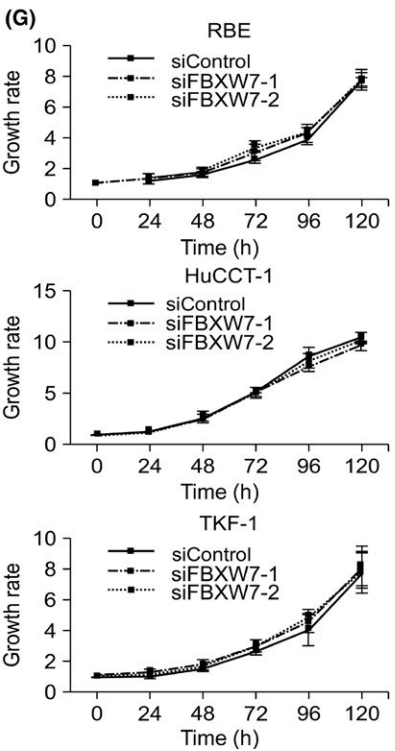
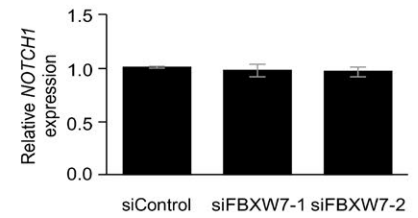
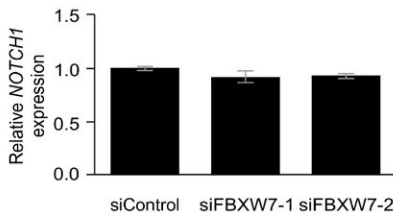
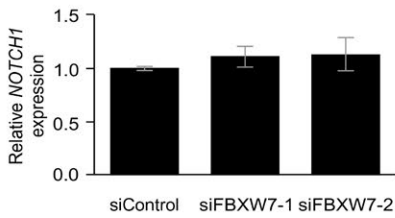
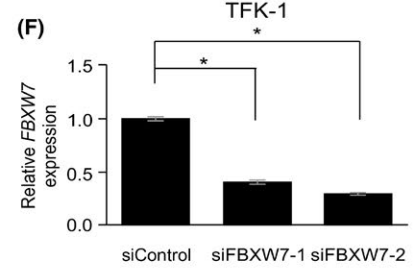
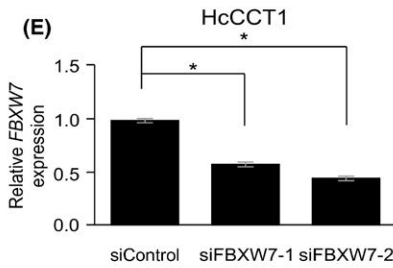
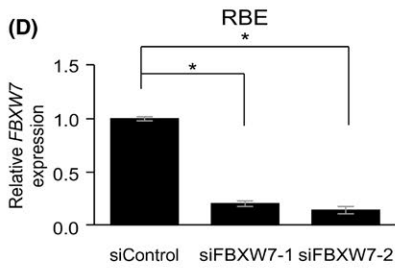
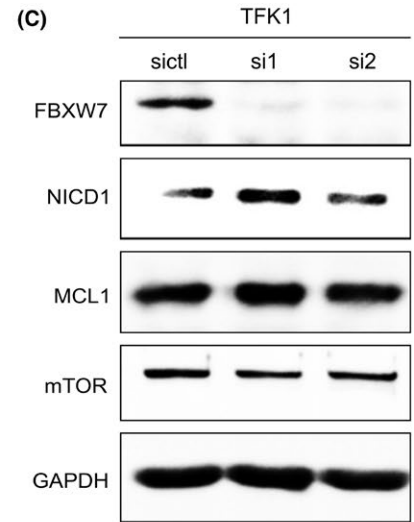
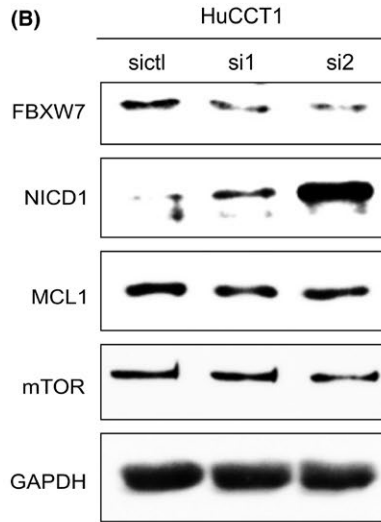
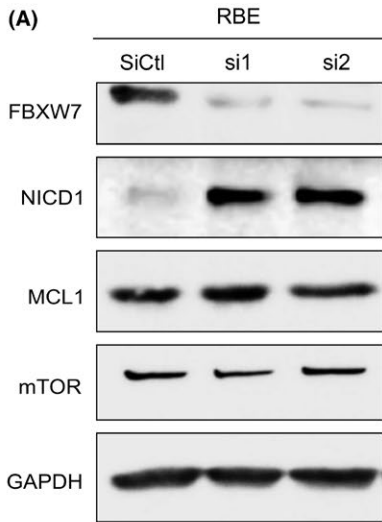


FIGURE 2 FBXW7 deficiency results in NOTCH1 intracellular domain (NICD1) accumulation in cholangiocarcinoma (CC) cells. A, Immunoblot analysis of FBXW7 substrates in RBE cells. B, Immunoblot analysis of FBXW7 substrates in HuCCT1 cells. C, Immunoblot analysis of FBXW7 substrates in TFK-1 cells. D, Evaluation of *FBXW7* and *NOTCH1* mRNA levels by quantitative (qRT-PCR) in RBE cells. E, Evaluation of *FBXW7* and *NOTCH1* mRNA levels by qRT-PCR in HuCCT1 cells. F, Evaluation of *FBXW7* and *NOTCH1* mRNA levels by qRT-PCR in TFK-1 cells. CC cell lines were treated with control siRNA (siControl) or siRNA targeting *FBXW7* (siFBXW7). G, Cell proliferation, as determined from RBE, HuCCT1, and TFK-1 cell growth curve analyses. CC cell lines were transfected with siControl or siFBXW7. H, Immunoblot analysis of FBXW7 substrates in RBE cells transfected with indicated shRNAs. I, Evaluation of *FBXW7* and *NOTCH1* mRNA levels by qRT-PCR in RBE cells transfected with indicated shRNAs. Results represent the mean of triplicate determinations. * $P < .05$ (Student's *t*-test). EV, empty vector; sh1, short hairpin *FBXW7*-1; sh2, short hairpin *FBXW7*-2; si1, short interfering *FBXW7*-1; si2, short interfering *FBXW7*-2; siCtl, short interfering control

those with relatively low expression (H score ≤ 110 , $n = 117$). There were no correlations between any clinicopathological features and FBXW7 expression levels in tumor tissue samples from CC patients (Table 1).

3.2 | FBXW7 expression is associated with CC patient survival

We evaluated patient survival using Kaplan-Meier survival analysis to compare the postoperative prognosis of patients with high vs low FBXW7 expression. The log-rank test revealed significant differences in DFS and OS between the two groups ($P = .001$ and $P < .001$, respectively) (Figure 1). Both DFS and OS rates were lower in patients with low FBXW7 expression than in those with high FBXW7 expression, with 5-year survival rates of 38.6% and 89.7%, respectively.

3.3 | FBXW7 expression is a prognostic biomarker in CC

To assess the prognostic value of FBXW7, we carried out univariate analyses for DFS and OS in CC patients. The univariate analysis for DFS revealed that FBXW7 expression ($P = .001$), UICC primary tumor classification (UICC-pT) ($P = .002$), UICC-pN ($P < .0001$), lymphatic invasion ($P = .0004$), venous invasion ($P = .01$), neural invasion ($P = .001$), and adjuvant chemotherapy ($P = .001$) were useful prognostic factors (Table 2A). Multivariate Cox regression analysis showed that FBXW7 expression ($P = .006$) and UICC-pN ($P < .0001$) were independent prognostic factors for DFS (Table 2A). The univariate analysis for OS revealed that FBXW7 expression ($P = .0001$), UICC-pT ($P = .001$), UICC-pN ($P < .0001$), UICC-pM ($P < .0001$), lymphatic invasion ($P = .013$), neural invasion ($P = .029$), curative resection ($P = .029$), and adjuvant chemotherapy ($P = .005$) were valuable prognostic factors (Table 2B). Multivariate Cox regression analysis indicated that FBXW7 expression ($P = .0004$), UICC-pT ($P = .032$), UICC-pN ($P = .001$), and UICC-pM ($P = .029$) were independent predictors of OS (Table 2B). These results show that, in addition to other reported factors,^{4,40} FBXW7 expression is a useful prognostic biomarker in CC patients.

3.4 | FBXW7 suppression leads to NOTCH1 accumulation

Immunohistochemical analysis of CC patient tissue samples revealed that low FBXW7 expression was significantly associated

with extremely poor prognosis. To determine whether FBXW7 suppression and the consequent accumulation of its substrates were the cause of poor outcomes, we examined the ubiquitin ligase function of FBXW7 in RBE, HuCCT1, and TFK-1 cells. In all 3 CC cell lines, NOTCH1 expression was upregulated following FBXW7 suppression (Figure 2A-C, Figure S2A-C), with no changes observed in the levels of MCL1, mTOR (Figure 2A-C, Figure S2A-C), cyclin E, c-Myc, or c-Jun (data not shown). In contrast, qRT-PCR analysis revealed that *NOTCH1* mRNA levels were unaltered in CC cells in which FBXW7 was suppressed (Figure 2D-F). These results indicate that NOTCH1 is regulated by FBXW7 not at the transcriptional but at the protein level; that is, suppression of FBXW7 results in the accumulation of NOTCH1 in CC cells.

3.5 | FBXW7 suppression does not affect CC cell proliferation

To investigate the role of FBXW7 in the progression of CC, we evaluated the effect of FBXW7 suppression on CC cell proliferation by counting the number of cells every 24 hours. There was no difference in the growth rates of FBXW7-depleted and control cells in any of the cell lines examined (Figure 2G).

3.6 | FBXW7 suppression promotes CC progression

We established stable silencing of FBXW7 in RBE cells by transfecting them with *FBXW7* shRNA. FBXW7 knockdown resulted in the accumulation of NOTCH1, as determined by immunoblotting (Figures 2H, S2D); however, qRT-PCR analysis revealed that the *NOTCH1* mRNA level was unaltered (Figure 2I). Similar results were obtained by siRNA-mediated FBXW7 knockdown.

Although low FBXW7 expression was linked to poor survival in CC patients, FBXW7 suppression did not affect CC cell proliferation. NOTCH signaling has been shown to promote self-renewal, differentiation, proliferation, survival, angiogenesis, and migration^{27,28}; therefore, as NOTCH1 is a substrate of FBXW7 in CC cells, we examined its role as an oncoprotein by evaluating whether NOTCH1 activation in FBXW7-depleted CC cells enhanced self-renewal and migration using colony formation, wound healing, and migration assays. FBXW7 inhibition increased colony number (Figure 3A) and promoted cell migration (Figure 3B,C) compared to levels in the control treatment. To determine whether these effects were attributable

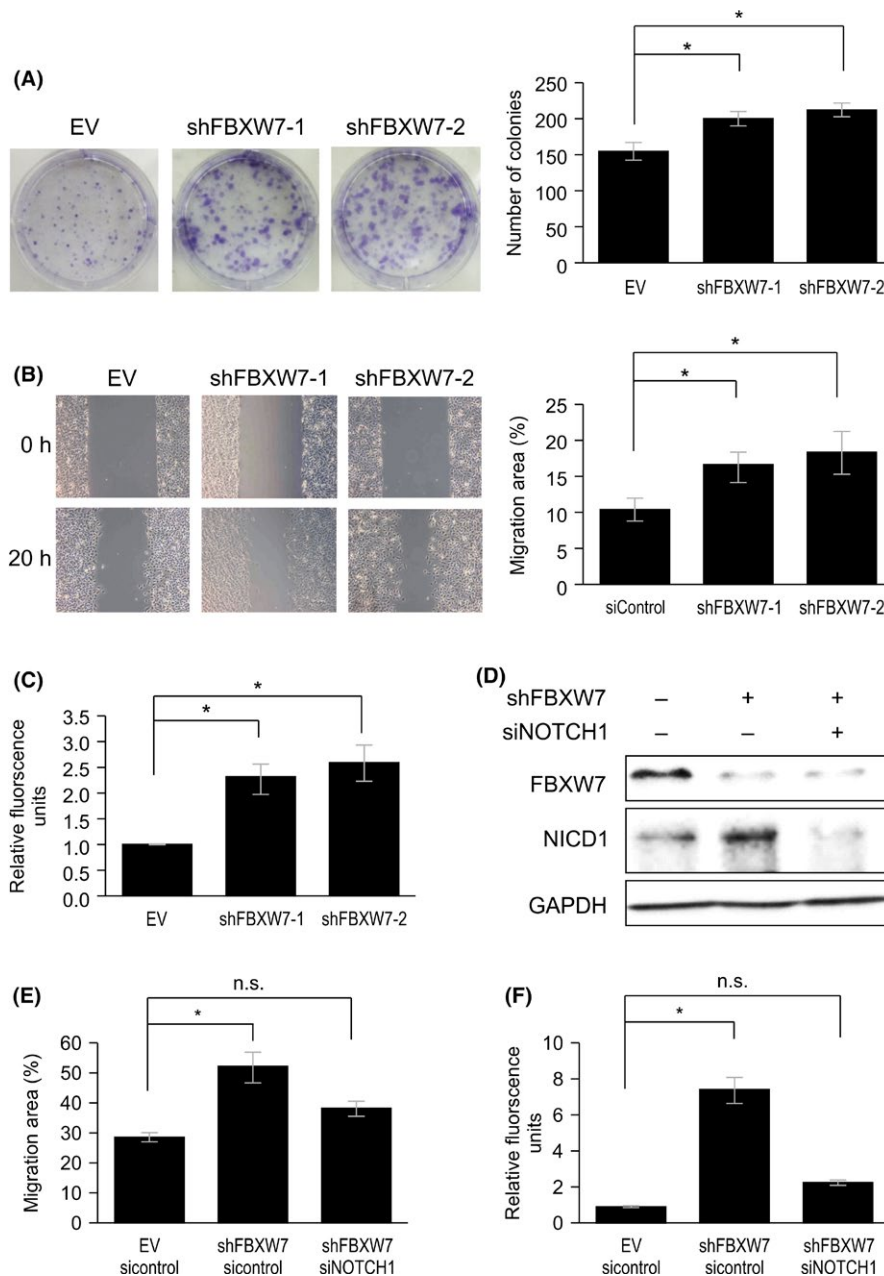


FIGURE 3 FBXW7 depletion promotes cholangiocarcinoma progression. A, Colony formation in FBXW7-depleted RBE cells. B,C, Migratory capacity of FBXW7-depleted RBE cells, as determined by wound healing assay (B) and Transwell migration assay (C). D, Immunoblot analysis of FBXW7 and NOTCH1 intracellular domain (NICD1) following inhibition of NOTCH1 in FBXW7-depleted RBE cells. E,F, Migratory capacity of FBXW7-depleted RBE cells following inhibition of NOTCH1, as determined by wound healing assay (E) and Transwell migration assay (F). Results in A-F show the mean of triplicate determinations. * $P < .05$ (Student's *t* test). EV, empty vector; sh1, short hairpin FBXW7-1; sh2, short hairpin FBXW7-2; si1, short interfering FBXW7-1; si2, short interfering FBXW7-2; siCtl, short interfering control

to NOTCH1 activation, we knocked down NOTCH1 in FBXW7-depleted CC cells (Figures 3D, S3). Loss of NOTCH1 attenuated the migratory capacity of CC cells, restoring control levels (Figure 3E,F). Consistent with previous reports,^{27,28,41} suppression of FBXW7 also enhanced the self-renewal of CC cells according to colony formation assay. Thus, FBXW7 inhibits CC cell migration through downregulation of NOTCH1.

3.7 | FBXW7 suppression inhibits CDDP-induced apoptosis through MCL1 accumulation

Cis-diamminedichloridoplatinum is a chemotherapeutic agent that is widely used to treat patients with CC.⁶ We examined the effect of FBXW7 suppression on CDDP-induced apoptosis. In cells without CDDP treatment, the rate of apoptosis was unaffected by FBXW7

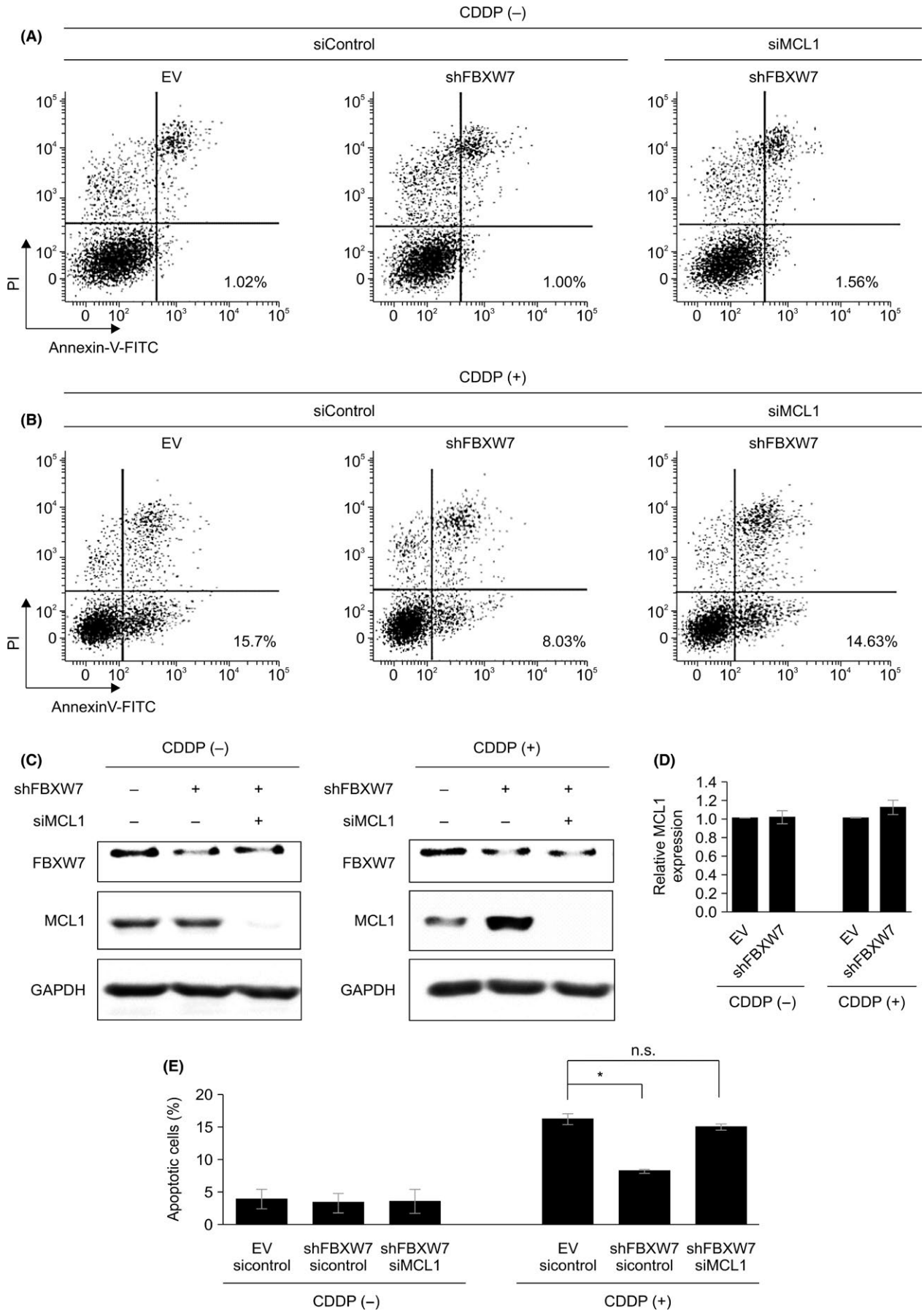


FIGURE 4 FBXW7 knockdown blocks cis-diamminedichloridoplatinum(II) (CDDP)-induced apoptosis through regulation of myeloid cell leukemia sequence 1 (MCL1). A,B, Proportion of apoptotic cells, as detected by flow cytometry, following CDDP treatment (50 $\mu\text{mol/L}$) of FBXW7-depleted RBE cells transfected with control siRNA (siControl) or siRNA targeting *MCL1* (siMCL1). C, Immunoblot analysis of FBXW7-depleted RBE cells transfected with siMCL1 or siControl and treated with 50 $\mu\text{mol/L}$ CDDP for 24 h. D, Quantitative RT-PCR analysis of relative *MCL1* mRNA levels in FBXW7-depleted RBE cells treated with 50 $\mu\text{mol/L}$ CDDP for 24 h or left untreated. Results represent the mean \pm SE of 3 independent experiments. * $P < .05$ (Student's *t* test)

knockdown (Figure 4A). However, in the presence of CDDP, the fraction of apoptotic cells was reduced in FBXW7-depleted CC cells compared to that in control cells (Figure 4B).

Myeloid cell leukemia sequence 1 is a FBXW7 substrate that is associated with CDDP resistance in several types of malignancy.^{36,38,42} To determine whether MCL1 is regulated by FBXW7 in CC cells treated with CDDP, we analyzed MCL1 levels in FBXW7-depleted CC cells by immunoblotting. We found that MCL1 expression was increased in these cells in the presence, but not in the absence, of CDDP (Figures 2A-C,H, 4C, S4A). In contrast, there was no change in MCL1 mRNA expression following suppression of FBXW7 (Figure 4D).

To determine whether MCL1 mediates the effects of FBXW7 on apoptosis, we silenced MCL1 in FBXW7-depleted CC cells, and we found that the apoptotic fraction was restored to control levels (Figure 4B,E). These results suggest that FBXW7 enhances apoptosis by promoting the degradation of MCL1 in CC.

4 | DISCUSSION

Among cancers, CC has one of the worst prognoses. As such, there is an urgent need to identify new prognostic biomarkers and therapeutic targets. The downregulation of FBXW7, which encodes a tumor-suppressor protein, is observed in various types of cancer and affects many aspects of carcinogenesis, including cell cycle progression, proliferation, differentiation, stem cell quiescence, transcription, DNA damage repair, and apoptosis.⁴³ Mutations in FBXW7 have been observed in various types of human cancer, including CC.^{9,20-24} In the absence of FBXW7 mutations, impairment of FBXW7 function by a mechanism involving activated Ras-Raf-MEK-ERK signaling is reportedly associated with tumorigenic potential and poor prognosis in pancreatic ductal cancer.²⁶ Furthermore, miR-223 promotes CDDP resistance in gastric cancer cells by regulating G_1/S cell cycle transition and apoptosis through the targeting of FBXW7.⁴² Therefore, we sought to confirm the association between low FBXW7 expression and poor prognosis in CC, regardless of mutation status.

In the present study, we determined that FBXW7 expression level was the most important independent prognostic factor for DFS and OS, although there were no correlations between any clinicopathological features and FBXW7 expression levels in tumor tissue samples from CC patients. Loss of FBXW7 has been linked to tumor progression and poor prognosis in intrahepatic CC⁴⁴; however, in this prior study, downregulation of FBXW7 was not identified as an independent prognostic factor for DFS or OS, most likely because of the small number of patients

included. Our results indicate that FBXW7 can predict malignant potential in CC and might be associated with sensitivity to therapy after recurrence.

The NOTCH signaling pathway is evolutionarily conserved and plays important roles in cell self-renewal, differentiation, proliferation, survival, angiogenesis, and migration.^{27,28} NOTCH signaling is aberrantly activated in various malignancies, including ovarian, breast, and pancreatic cancers and leukemia.²⁹⁻³² NOTCH signaling is also activated in CC, and NOTCH overexpression has been linked to poor survival.³⁵ NOTCH signaling could induce a biliary differentiation program in hepatocytes or hepatic progenitor cells, resulting in intrahepatic CC.³⁴ In the present study, we observed NOTCH1 accumulation in CC cells depleted of FBXW7. It was recently shown that increases in colony-forming capacity, invasiveness, and migratory ability were associated with other CSC characteristics, such as self-renewal, in hepatocellular carcinoma and promoted tumor initiation and growth, leading to metastasis.⁴¹ In addition, it was reported that suppression of FBXW7 increased the expression of OCT4 and NANOG in CC cells and that the cells formed tumor spheres, which indicated promotion of the CSC-like capability of CC cells.¹⁶ The increased self-renewal capacity observed in our study could be due to NOTCH1 accumulation resulting from FBXW7 suppression in CC. Moreover, FBXW7 knockdown induced CC cell migration by an increase in NOTCH1, which could promote malignant potential and metastasis in CC. In contrast, previous experiments by our group have shown that there were no significant survival differences between patients with and without NOTCH1 expression. Thus, we concluded that the relationships between the clinicopathological features of CC and NOTCH differed according to the type of NOTCH receptors and that NOTCH signaling participates in the initial step of tumor progression.³⁵

The current standard for chemotherapy in advanced and recurrent CC is the combination of GEM and CDDP,⁶ but its efficacy is limited due to the development of chemoresistance, the mechanisms of which are not well understood. Several studies have, however, described the relationship between CDDP resistance and the accumulation of MCL1.³⁶⁻³⁸ Unlike other B-cell lymphoma two family members, MCL1 is unstable⁴⁵ and provides a mechanism for cells to shift from survival to apoptosis in response to stressors.⁴⁶ FBXW7 modulates the apoptotic pathway by regulating MCL1 degradation.¹² However, the relationship between the FBXW7/MCL1 pathway and CDDP-induced apoptosis in CC has not been previously investigated. We reveal here for the first time that suppression of FBXW7 inhibits CDDP-induced apoptosis by accumulation of MCL1 in CC. We found that MCL1 was a

substrate of FBXW7 only in CC cells that were stimulated with CDDP and that FBXW7-depleted CC cells with increased MCL1 expression were less sensitive to apoptotic signals. Moreover, inhibiting MCL1 expression in FBXW7-depleted cells restored apoptosis to control levels. Collectively, these data suggest that FBXW7-deficient CC cells require elevated levels of MCL1 to evade apoptosis. MCL1 accumulation resulting from reduced FBXW7 expression could thus contribute to a decrease in OS associated with resistance to CDDP-based chemotherapy. In tumor tissue samples from CC patients who received or did not receive CDDP, however, FBXW7 expression was not an independent prognostic factor for OS, likely because of the small number of high-FBXW7 patients who were treated with CDDP, which is a limitation of this retrospective analysis. Additionally, there were no significant inverse associations between FBXW7 expression and MCL1 expression by Pearson's correlation analysis. Our results showed that MCL1 was a substrate of FBXW7 only in CC cells stimulated with CDDP and that FBXW7-depleted CC cells with increased MCL1 expression were less sensitive to apoptotic signals, which did not contradict the results of immunohistochemical analysis. Thus, it seems useful to prospectively analyze tissue samples from unresectable CC patients. In addition, MCL1 accumulation and function were dependent on CDDP stimulation; this is in accordance with other reports that MCL1 is extremely unstable in nature and is affected by various stresses.^{45,46} For example, FBXW7-deficient human T-ALL cells with elevated MCL1 expression are more sensitive to a multikinase inhibitor than T-ALL cell lines with WT FBXW7 levels.¹² Moreover, Nakajima et al showed that CDDP transcriptionally induced Noxa, which enhanced MCL1 phosphorylation, ubiquitination, and proteasome-mediated degradation.³⁷ Thus, in the present study, we found that the phosphorylation of MCL1 was upregulated by CDDP treatment, which affected the FBXW7/MCL1 interaction. However, we could not identify the specific molecules that enhanced CDDP-induced MCL1 phosphorylation. Therefore, further studies are needed to verify the mechanisms of MCL1 accumulation and function that are dependent on CDDP stimulation.

An association between the downregulation of FBXW7 and accumulation of its substrates has been reported in various malignancies.¹²⁻¹⁸ In CC, mTOR is a substrate of FBXW7 that is implicated in epithelial-mesenchymal transition and metastasis.¹⁶ However, we did not observe any increases in the levels of mTOR or other reported FBXW7 substrates in CC cells transfected with either siRNA or shRNA against FBXW7. It has been reported that FBXW7 ubiquitylation of its substrates is context- and tissue-dependent.^{9,47-49} Thus, similar to the accumulation of MCL1 in response to CDDP, an increase in the other FBXW7 substrates might be observed in specific tissues or contexts.

To evaluate the effect of FBXW7 on GEM-induced apoptosis, we analyzed the apoptotic rate in CC cells treated with GEM. Gemcitabine did not induce apoptosis in a concentration-dependent manner (Figure S4B). It was previously reported that GEM-resistant pancreatic cancer cells show senescence-associated phenotypes instead of undergoing

apoptosis, leading to reversible cellular arrest to evade cell death and the development of GEM resistance.⁵⁰ We propose that a similar phenomenon occurs in CC cells treated with GEM.

In this study, we identified NOTCH1 and MCL1 as two substrates of FBXW7 in CC cells. Although it is important to understand the interaction between NOTCH1 and MCL1, this was not investigated here and will be addressed in future studies. Moreover, it has been reported that impairment of FBXW7 function by a mechanism involving activated Ras is associated with tumorigenic potential and poor prognosis²⁶ and that the *Fbxw7* gene is a p53-dependent tumor-suppressor gene in mice.¹⁵ Thus, FBXW7 might be associated with other tumor and tumor-suppressor genes that might contribute to poor prognosis of CC.

In conclusion, our study showed that suppression of FBXW7 is associated with poor survival outcome in CC patients. FBXW7 was found to regulate the migration and self-renewal of CC cells through modulation of NOTCH1 as well as CDDP-induced apoptosis by MCL1 accumulation in CC cells. These findings suggest that FBXW7 modulates the malignant potential—including metastasis and chemoresistance—of CC through two signals, NOTCH1 and MCL1. Moreover, FBXW7 is a potential biomarker and therapeutic target for the treatment of CC.

ACKNOWLEDGMENTS

We thank Professor Keiko Nakayama and Dr. Ryo Funayama of the Department of Cell Proliferation, Tohoku University Graduate School of Medicine; Yayoi Aoyama of the Department of Pathology, Tohoku University Hospital; and Emiko Shibuya and Keiko Inabe of the Department of Surgery, Tohoku University Graduate School of Medicine, for providing technical support. This study was supported by a Grant-in-Aid for Young Scientists (B) (grant no. 26861058 and 16K19910) from the Japan Society for the Promotion of Science.

DISCLOSURE

The authors have no conflict of interests.

ORCID

Kunihiko Masuda  <http://orcid.org/0000-0001-6879-5899>

REFERENCES

1. Tyson GL, Ilyas JA, Duan Z, et al. Secular trends in the incidence of cholangiocarcinoma in the USA and the impact of misclassification. *Dig Dis Sci*. 2014;59:3103-3110.
2. Tyson GL, El-Serag HB. Risk factors for cholangiocarcinoma. *Hepatology*. 2011;54:173-184.
3. Rizvi S, Gores GJ. Pathogenesis, diagnosis, and management of cholangiocarcinoma. *Gastroenterology*. 2013;145:1215-1229.
4. Unno M, Katayose Y, Rikiyama T, et al. Major hepatectomy for perihilar cholangiocarcinoma. *J Hepatobiliary Pancreat Sci*. 2010;17:463-469.

5. Shirai K, Ebata T, Oda K, et al. Perineural invasion is a prognostic factor in intrahepatic cholangiocarcinoma. *World J Surg.* 2008;32:2395-2402.
6. Valle J, Wasan H, Palmer DH, et al. Cisplatin plus gemcitabine versus gemcitabine for biliary tract cancer. *N Engl J Med.* 2010;362:1273-1281.
7. Zhao DY, Lim KH. Current biologics for treatment of biliary tract cancers. *J Gastrointest Oncol.* 2017;8:430-440.
8. Sundaram M, Greenwald I. Suppressors of a lin-12 hypomorph define genes that interact with both lin-12 and glp-1 in *Caenorhabditis elegans*. *Genetics.* 1993;135:765-783.
9. Nakayama KI, Nakayama K. Ubiquitin ligases: cell-cycle control and cancer. *Nat Rev Cancer.* 2006;6:369-381.
10. Welcker M, Clurman BE. FBW7 ubiquitin ligase: a tumour suppressor at the crossroads of cell division, growth and differentiation. *Nat Rev Cancer.* 2008;8:83-93.
11. Oberg C, Li J, Pauley A, Wolf E, Gurney M, Lendahl U. The Notch intracellular domain is ubiquitinated and negatively regulated by the mammalian Sel-10 homolog. *J Biol Chem.* 2001;276:35847-35853.
12. Inuzuka H, Shaik S, Onoyama I, et al. SCF^{FBW7} regulates cellular apoptosis by targeting MCL1 for ubiquitylation and destruction. *Nature.* 2011;471:104-109.
13. Koepp DM, Schaefer LK, Ye X, et al. Phosphorylation-dependent ubiquitination of cyclin E by the SCFFbw7 ubiquitin ligase. *Science.* 2001;294:173-177.
14. Tetzlaff MT, Yu W, Li M, et al. Defective cardiovascular development and elevated cyclin E and Notch proteins in mice lacking the Fbw7 F-box protein. *Proc Natl Acad Sci USA.* 2004;101:3338-3345.
15. Mao JH, Kim IJ, Wu D, et al. FBXW7 targets mTOR for degradation and cooperates with PTEN in tumor suppression. *Science.* 2008;321:1499-1502.
16. Yang H, Lu X, Liu Z, et al. FBXW7 suppresses epithelial-mesenchymal transition, stemness and metastatic potential of cholangiocarcinoma cells. *Oncotarget.* 2015;6:6310-6325.
17. Welcker M, Orian A, Grim JE, Eisenman RN, Clurman BE. A nuclear isoform of the Fbw7 ubiquitin ligase regulates c-Myc and cell size. *Curr Biol.* 2004;14:1852-1857.
18. Yada M, Hatakeyama S, Kamura T, et al. Phosphorylation-dependent degradation of c-Myc is mediated by the F-box protein Fbw7. *EMBO J.* 2004;23:2116-2125.
19. Nateri AS, Riera-Sans L, Da Costa C, Behrens A. The ubiquitin ligase SCFFbw7 antagonizes apoptotic JNK signaling. *Science.* 2004;303:1374-1378.
20. Wood LD, Parsons DW, Jones S, et al. The genomic landscapes of human breast and colorectal cancers. *Science.* 2007;318:1108-1113.
21. Maser RS, Choudhury B, Campbell PJ, et al. Chromosomally unstable mouse tumours have genomic alterations similar to diverse human cancers. *Nature.* 2007;447:966-971.
22. Akhoondi S, Sun D, von der Lehr N, et al. FBXW7/hCDC4 is a general tumor suppressor in human cancer. *Cancer Res.* 2007;67:9006-9012.
23. Lee H, Wang K, Johnson A, et al. Comprehensive genomic profiling of extrahepatic cholangiocarcinoma reveals a long tail of therapeutic targets. *J Clin Pathol.* 2016;69:403-408.
24. Churi CR, Shroff R, Wang Y, et al. Mutation profiling in cholangiocarcinoma: prognostic and therapeutic implications. *PLoS ONE.* 2014;9:e115383.
25. Davis RJ, Welcker M, Clurman BE. Tumor suppression by the Fbw7 ubiquitin ligase: mechanisms and opportunities. *Cancer Cell.* 2014;26:455-464.
26. Ji S, Qin Y, Shi S, et al. ERK kinase phosphorylates and destabilizes the tumor suppressor FBW7 in pancreatic cancer. *Cell Res.* 2015;25:561-573.
27. Kopan R, Ilgan MX. The canonical Notch signaling pathway: unfolding the activation mechanism. *Cell.* 2009;137:216-233.
28. Fortini ME. Notch signaling: the core pathway and its posttranslational regulation. *Dev Cell.* 2009;16:633-647.
29. Cancer Genome Atlas Research Network. Integrated genomic analyses of ovarian carcinoma. *Nature.* 2011;474:609-615.
30. Acar A, Simoes BM, Clarke RB, Brennan K. A role for Notch signalling in breast cancer and endocrine resistance. *Stem Cells Int.* 2016;2016:2498764.
31. Miyamoto Y, Maitra A, Ghosh B, et al. Notch mediates TGF α -induced changes in epithelial differentiation during pancreatic tumorigenesis. *Cancer Cell.* 2003;3:565-576.
32. Weng AP, Ferrando AA, Lee W, et al. Activating mutations of NOTCH1 in human T cell acute lymphoblastic leukemia. *Science.* 2004;306:269-271.
33. Mansour MR, Sulis ML, Duke V, et al. Prognostic implications of NOTCH1 and FBXW7 mutations in adults with T-cell acute lymphoblastic leukemia treated on the MRC UKALLXII/ECOG E2993 protocol. *J Clin Oncol.* 2009;27:4352-4356.
34. Zender S, Nischeleit I, Wuestefeld T, et al. A critical role for Notch signaling in the formation of cholangiocellular carcinomas. *Cancer Cell.* 2013;23:784-795.
35. Aoki S, Mizuma M, Takahashi Y, et al. Aberrant activation of Notch signaling in extrahepatic cholangiocarcinoma: clinicopathological features and therapeutic potential for cancer stem cell-like properties. *BMC Cancer.* 2016;16:854.
36. Li Q, Zhan M, Chen W, et al. Phenylethyl isothiocyanate reverses cisplatin resistance in biliary tract cancer cells via glutathionylation-dependent degradation of Mcl-1. *Oncotarget.* 2016;7:10271-10282.
37. Nakajima W, Sharma K, Lee JY, et al. DNA damaging agent-induced apoptosis is regulated by MCL-1 phosphorylation and degradation mediated by the Noxa/MCL-1/CDK2 complex. *Oncotarget.* 2016;7:36353-36365.
38. Ma J, Zhao Z, Wu K, Xu Z, Liu K. MCL-1 is the key target of adjuvant chemotherapy to reverse the cisplatin-resistance in NSCLC. *Gene.* 2016;587:147-154.
39. Azim HA Jr, Peccatori FA, Brohee S, et al. RANK-ligand (RANKL) expression in young breast cancer patients and during pregnancy. *Breast Cancer Res.* 2015;17:24.
40. Seyama Y, Kubota K, Sano K, et al. Long-term outcome of extended hemihepatectomy for hilar bile duct cancer with no mortality and high survival rate. *Ann Surg.* 2003;238:73-83.
41. Luo J, Wang P, Wang R, et al. The Notch pathway promotes the cancer stem cell characteristics of CD90+ cells in hepatocellular carcinoma. *Oncotarget.* 2016;7:9525-9537.
42. Zhou X, Jin W, Jia H, Yan J, Zhang G. MiR-223 promotes the cisplatin resistance of human gastric cancer cells via regulating cell cycle by targeting FBXW7. *J Exp Clin Cancer Res.* 2015;34:28.
43. Schwartz AL, Ciechanover A. Targeting proteins for destruction by the ubiquitin system: implications for human pathobiology. *Ann Rev Pharmacol Toxicol.* 2009;49:73-96.
44. Enkhbold C, Utsunomiya T, Morine Y, et al. Loss of FBXW7 expression is associated with poor prognosis in intrahepatic cholangiocarcinoma. *Hepatol Res.* 2014;44:E346-E352.
45. Maurer U, Charvet C, Wagman AS, DeJardin E, Green DR. Glycogen synthase kinase-3 regulates mitochondrial outer membrane permeabilization and apoptosis by destabilization of MCL-1. *Mol Cell.* 2006;21:749-760.
46. Opferman JT, Letai A, Beard C, Sorcinelli MD, Ong CC, Korsmeyer SJ. Development and maintenance of B and T lymphocytes requires antiapoptotic MCL-1. *Nature.* 2003;426:671-676.
47. Kourtis N, Moubarak RS, Aranda-Orgilles B, et al. FBXW7 modulates cellular stress response and metastatic potential through HSF1 post-translational modification. *Nat Cell Biol.* 2015;17:322-332.
48. Masuda K, Ishikawa Y, Onoyama I, et al. Complex regulation of cell-cycle inhibitors by Fbxw7 in mouse embryonic fibroblasts. *Oncogene.* 2010;29:1798-1809.
49. Balamurugan K, Wang JM, Tsai HH, et al. The tumour suppressor C/EBP δ inhibits FBXW7 expression and promotes mammary tumour metastasis. *EMBO J.* 2010;29:4106-4117.

50. Song Y, Baba T, Mukaida N. Gemcitabine induces cell senescence in human pancreatic cancer cell lines. *Biochem Biophys Res Comm.* 2016;477:515-519.

SUPPORTING INFORMATION

Additional supporting information may be found online in the Supporting Information section at the end of the article.

How to cite this article: Mori A, Masuda K, Ohtsuka H, et al. FBXW7 modulates malignant potential and cisplatin-induced apoptosis in cholangiocarcinoma through NOTCH1 and MCL1. *Cancer Sci.* 2018;109:3883-3895. <https://doi.org/10.1111/cas.13829>